

DYNAMIC ANALYSIS OF A GAS-SOLID FLUIDIZED-BED GASIFIER FOR FULL GAS PRODUCTION FROM BIOMASS

Silva, J. D.

Federal University of Pernambuco, UFPE, Artur de Sá, 50740-521, Recife - PE Brazil, control and optimization process
Laboratory, Phone number: (0-XX-81) 2126-7270, Fax: (0-XX-81) 2126-7274, e-mail jornandesdias@yahoo.com.br

Abstract. The technology of the gas-solid fluidized-bed gasifier can be developed to convert solid fuel in to electric energy through the gasification process. The gas-solid fluidized-bed analyzed in this work involves ascending air-steam phases and a descending solid fuel. The mathematical modeling developed for this process is composed of energy balance equations and of the balance equations of the chemical species. This equation set forms a coupled partial differential equation (PDEs) system. The solution of this equation system was accomplished with the algorithm of the method of lines. The PDEs system was transformed in to a coupled ordinary differential equation (ODEs) system. The ODEs system was solved with the implementation of the Runge-Kutta Gill method, using a computer program developed in Fortran 90 language. The numeric experiments were analyzed through temperatures profiles, as well as profiles of the chemical species that compose the gasification process in the fluidized-bed gasifier. The numeric experiments were validated with experimental data to test the precision, convergence and stability.

Keywords: gas-solid, fluidized bed, gasification, biomass, full

1. INTRODUCTION

The strategic politics of the Brazilian electric sector foresees an amplification of the electric energy production from renewable sources. However, the electric energy production from the gasification of biomassing solid wastes is a promising alternative technology for this sector. This technology involves an integration process, fluidized-bed gasifier (FBG)/gas turbine (GT), which can be configured by a simple integration, that is, hardly a GT integrated to FBG or through combined cycle (Brayton/Rankine) that includes the integration of a GT and a steam turbine (ST) integrated to FBG (Gabra et al., 2001a, b, c).

The technology of the biomass gasification in a FBG needs of the detailed knowledge of the physical and chemical phenomenon to optimize the energy efficiency in the gasifier. However, the mathematical models are important tools to investigate these physical and chemical phenomenon that happen in the FBG. Usually, The mathematical models are composed by moment, energy and mass balance equations. In the present work, it was just studied the energy and mass balance equations.

The FBG for a simple cycle plant or for a combined cycle plant is equipment with complex operation. Therefore, the operational control of the gasification reactions is difficult task. The referring mass balance equations to each component (reagents and products) of the gasification process compose the mathematical modelling for the FBG. The mathematical modelling developed for the FBG was used to simulate the behavior of the components of the gasification reactions, as well as the thermal behavior in the FBG.

The energy and mass balance equations developed for the gasification process form a coupled partial differential equation (PDEs) system. The numerical solution of this PDEs system was accomplished with implementation of Runge-Kutta Gill method (Silva et al, 2002a, 2004b).

The cane bagasse is a promising solid fuel for the power generation system in FBG with high efficiency and at low cost (Gabra et al., 2001, Bridgewater, 1995). Before the gasification process to be accomplished, the cane bagasse suffers a pre-treatment as the following steps: (i) the cane bagasse is briquetted; (ii) drying to evaporate moisture; (iii) it should be heated up to 300°C-500°C.

The gasification process involves the solid fuel entrance in the top of the FBG and the air and steam entrance in the base of the FBG. In the gasification zone happens homogeneous and heterogeneous reactions.



Therefore, the objective of this work is to analyze the behavior of the resulting components (C, CO, O₂, H₂, CO₂, H₂O) of the gasification process through the modelling and simulation.

2. DEVELOPMENT OF THE PHYSICAL MODELLING FOR THE GASIFICATION PROCESS

Usually, fluidized-bed gasifier (FBG) is divided in two zones: (i) a fluid-solid fluidization zone; (ii) a solid free zone (Freeboard). The mathematical modelling developed for this work was just restricted to fluid-solid fluidization zone. In this zone, it will happen the combustion and gasification reactions. The Figure 1 shows a prototype simplified of the FBG that will be used for the simulation of this work.

- Balances for the gaseous species O₂, CO, CO₂, H₂O and H₂.

$$\frac{\partial(\varepsilon_g \rho_g Y_i)}{\partial t} + \frac{Q_g}{A_s} \frac{\partial(\varepsilon_g \rho_g Y_i)}{\partial z} = D_{i, \text{eff}} \frac{\partial^2(\varepsilon_g \rho_g Y_i)}{\partial z^2} + \frac{R T_g}{P} R_i; i=O_2, CO, CO_2, H_2O \text{ and } H_2 \quad (9)$$

- Initial and boundary conditions;

$$Y_i|_{t=0} = 0 \quad (10)$$

$$D_{i, \text{eff}} \frac{\partial(\varepsilon_g \rho_g Y_i)}{\partial z} \Big|_{z=0^+} = \frac{Q_g}{A_s} \left[(\varepsilon_g \rho_g Y_i) \Big|_{z=0^+} - (\varepsilon_g \rho_g Y_i) \Big|_{z=0^-} \right] \quad (11)$$

$$\frac{\partial(\varepsilon_g \rho_g Y_i)}{\partial z} \Big|_{z=H} = 0 \quad (12)$$

The C that appears in the heterogeneous chemical reactions is given in function of the burns rate of the individual C particles (Basu, 1999).

$$\frac{\partial(\varepsilon_s \rho_s Y_C)}{\partial t} + \frac{F_s}{A_s} \frac{\partial(\varepsilon_s \rho_s Y_C)}{\partial z} = D_{C, \text{eff}} \frac{\partial^2(\varepsilon_g \rho_g Y_C)}{\partial z^2} - 3 \frac{R T_g}{P} R_C \quad (13)$$

- Initial and boundary conditions;

$$Y_C|_{t=0} = 0 \quad (14)$$

$$D_{C, \text{eff}} \frac{\partial(\varepsilon_g \rho_g Y_C)}{\partial z} \Big|_{z=0^+} = \frac{F_s}{A_s} \left[(\varepsilon_g \rho_g Y_C) \Big|_{z=0^+} - (\varepsilon_g \rho_g Y_C) \Big|_{z=0^-} \right] \quad (15)$$

$$\frac{\partial(\varepsilon_g \rho_g Y_C)}{\partial z} \Big|_{z=H} = 0 \quad (16)$$

3. MATHEMATICAL MODELLING FOR THE KINETICS

The chemical equation system presented by the I to IV reactions couples one homogeneous reaction and three heterogeneous reactions. The I, II and IV reactions were classified as heterogeneous reactions, while the III reaction was classified as homogeneous. In the Table 1, the corresponding rates for each one of these reactions were presented:

Table-1: Kinetic rates for the I, II, III and IV reactions, References

Reactions Rates	References
$R_I = 6,0 \times 10^7 \left(\frac{Y_{O_2}}{2} \right) \exp\left(-\frac{29.790}{T_s} \right)$	Calleja et al (1981)
$R_{II} = 14,4 \text{ S} \exp\left(\frac{-166.156}{RT} \right) C_{H_2O}^{0,83} (1000)^{-0,17} \varepsilon_c$	Jong <i>et al</i> (2003)
$R_{III} = 1,3 \times 10^{11} \phi \left(\frac{RT_g}{P} \right)^{1/2} \left(\frac{Y_{O_2}}{2} \right)^{1/2} \exp\left(-\frac{15098}{T_s} \right)$	Ross e Davidson (1982)
$R_I = 3,0 \times 10^5 \left(\frac{Y_{O_2}}{2} \right) \exp\left(-\frac{17966}{T_s} \right)$	Calleja et al (1981)

The total rates of each component for consumption and production can be obtained using the following equation (Xiu et al, 2002).

$$r_i = \sum_{j=1}^3 v_{ij} R_j \quad (17)$$

where v_{ij} is the stoichiometric coefficient of the component i in the reaction j . The v_{ij} is negative for the reagent component. On the other hand, the v_{ij} is positive for the product component. Therefore, the total rate for each component was found as:

$$R_{O_2} = -R_I \quad (18)$$

$$R_{CO_2} = (R_I + R_{III}) - R_{IV} \quad (19)$$

$$R_{CO} = (R_{II} - R_{III}) + 2R_{IV} \quad (20)$$

$$R_{H_2} = R_{II} + R_{III} \quad (21)$$

$$R_{H_2O} = -(R_{II} + R_{III}) \quad (22)$$

The molar fraction of carbon that appears in the reactions I, II and IV is calculated with relation the combustion of the individual particles of carbon (Basu, 1999). The rate of carbon (RC) of Equation (29) was given by shrinking unreacted model (Levenspiel, 1984). The rate for this model was given by Basu and Fraser (1991) as:

$$R_C = \frac{P V_{O_2}}{T_g} \left(\frac{k_m k_c}{k_c + k_m} \right) Y_{O_2} \quad (23)$$

where,

$$k_m = 12 \frac{\phi Sh D_{O_2}}{d_c R T_m}; k_c = 1,006 \exp\left(-\frac{7137}{T_s}\right)$$

4. NUMERIC METHODOLOGY FOR THE MODEL

Equations of the model together with the total rates for the consumption and formation components form a coupled nonlinear EDPs system, which characterize an initial and boundary value problem. The PDEs system was transformed in a coupled ordinary differential equation (ODEs) system with implementation of the difference method finite to discrete the spatial derivatives.

- discretizing energy balance for the gaseous phase;

$$\frac{d(T_g)_j(t)}{dt} = \frac{\lambda_{g,eff}}{\rho_g C_{p,g} (\Delta z)^2} \left[(T_g)_{j+1}(t) - 2(T_g)_j(t) + (T_g)_{j-1}(t) \right] - \frac{Q_{ar}}{2\rho_g \Delta z} \left[(T_g)_{j+1}(t) - (T_g)_{j-1}(t) \right] - \frac{\varepsilon_s h_{gs}}{\varepsilon_g \rho_g C_{p,g}} \left[(T_g)_j(t) - (T_s)_j(t) \right] + \frac{(-\Delta H_{r,3})}{\varepsilon_g \rho_g C_{p,g}} (R_{3,g})_j \quad (24)$$

- discretizing initial and boundary conditions;

$$(T_g)_{j-1}(t) = 0 \quad (25)$$

$$(T_g)_{j+1}(t) = \frac{(2+\alpha_1)(T_g)_j(t) - 2\alpha_1 T_g|_{z=0^-}}{(2-\alpha_1)} \quad (26)$$

$$(T_g)_{N-1}(t) = (T_g)_N(t) \quad (27)$$

- discretizing energy balance for the solid phase;

$$\frac{d(T_s)_j(t)}{dt} = \frac{\lambda_{s,eff}}{\rho_s C_{p,s} (\Delta z)^2} \left[(T_s)_{j+1}(t) - 2(T_s)_j(t) + (T_s)_{j-1}(t) \right] - \frac{F_{t,s}}{2A_s \Delta z} \left[(T_s)_{j+1}(t) - (T_s)_{j-1}(t) \right] + \frac{h_{gs}}{\rho_s C_{p,s}} \left[(T_s)_j(t) - (T_g)_j(t) \right] - \frac{1}{\varepsilon_s C_{p,s}} \sum_{i=1}^3 (-\Delta H_{r,i}) (R_{r,i})_j(t) \quad (28)$$

- discretizing initial and boundary conditions;

$$(T_s)_{j-1}(t) = 0 \quad (29)$$

$$(T_s)_{j+1}(t) = \frac{(2+\alpha_2)(T_s)_j(t) - 2\alpha_2 T_s|_{z=0^-}}{(2-\alpha_2)} \quad (30)$$

$$(T_s)_{N-1}(t) = (T_s)_N(t) \quad (31)$$

- discretizing mass balance for the gaseous species O₂, CO, CO₂, H₂O and H₂;

$$\frac{d(Y_i)_j(t)}{dt} = \frac{D_{i,eff}}{(\Delta z)^2} \left[(Y_i)_{j+1}(t) - 2(Y_i)_j(t) + (Y_i)_{j-1}(t) \right] - \frac{Q_g}{2A_s \Delta z} \left[(Y_i)_{j+1}(t) - (Y_i)_{j-1}(t) \right] - \eta_{e,i} R \frac{(T_g)_j(t)}{P \varepsilon_g \rho_g} (R_i)_j(t); i = O_2, CO, CO_2, H_2O \text{ and } H_2 \quad (32)$$

- discretizing initial and boundary conditions;

$$(Y_i)_{j-1}(t) = 0 \quad (33)$$

$$(Y_i)_{j+1}(t) = \frac{(2+\beta_1)}{(2-\beta_1)} \left[(Y_i)_j(t) - 2\beta_1 Y_i(t) \Big|_{z=0^-} \right] \quad (34)$$

$$(Y_i)_{N-1}(t) = (Y_i)_N(t) \quad (35)$$

- discretizing mass balance for C;

$$\frac{d(Y_C)_j(t)}{dt} = \frac{D_{C,eff}}{(\Delta z)^2} \left[(Y_C)_{j+1}(t) - 2(Y_C)_j(t) + (Y_C)_{j-1}(t) \right] - \frac{F_{t,s}}{2A_s \Delta z} \left[(Y_C)_{j+1}(t) - (Y_C)_{j-1}(t) \right] - \frac{3}{\varepsilon_s} (R_C)_j(t) \quad (36)$$

- discretizing initial and boundary conditions;

$$(Y_C)_{j-1}(t) = 0 \quad (37)$$

$$(Y_C)_{j+1}(t) = \frac{(2+\beta_4)}{(2-\beta_4)} \left[(Y_C)_j(t) - 2\beta_4 Y_C(t) \Big|_{z=0^-} \right] \quad (38)$$

$$(Y_C)_{N-1}(t) = (Y_C)_N(t) \quad (39)$$

The parameters α_1 ; α_2 ; β_1 ; β_2 ; β_3 ; β_4 and the initial conditions are presented in the Table A1 of the Appendix A.

5. RESULTS AND DISCUSSIONS

Equations (24)-(39) were solved with application of the Runge-Kutta Gill method (Rice and Do, 1995). In sequence, it was developed a program in the Fortran 90 language to delimit T_g , T_s , Y_{O_2} , Y_{CO} , Y_{CO_2} , Y_{H_2O} and Y_C . The program was fed with the numerical values of the Table 2.

Table 2: data used in the simulation

Correlation	References
$V_{mf} = \frac{V_g}{d_s \rho_g} \left\{ \left[(25,25)^2 + \frac{0,0651 d_s^2 (\rho_s - \rho_g)^2 g}{\mu_g^2} \right]^{1/2} - 25,25 \right\}$	Sit e Grace, (1981)
$\varepsilon_s = \varepsilon_{mf} + 6,10 \times 10^{-4} \exp\left(\frac{V_{sg} - V_{mf}}{0,262}\right); \varepsilon_g = 0,784 - 0,139 \exp\left(\frac{V_{sg} - V_{mf}}{0,272}\right)$	Cui et al., (2000)
$\varepsilon_{mf} = 0,586 \left(\frac{1}{Ar}\right)^{0,029} \left(\frac{\rho_g}{\rho_s}\right)^{0,021}$	Broadhurst e Becker (1975)
$Nu_s = (7 - 10 \varepsilon_g + 5 \varepsilon_g^2) \left(1 + 0,7 Re_s^{0,2} Pr^{1/3}\right) + Re_s^{0,7} Pr^{1/3}$ $\left(1,33 - 2,4 \varepsilon_g + 1,2 \varepsilon_g^2\right)$	Syamlal et al., (1993)
$Ar = \rho_g (\rho_s - \rho_g) g \frac{d_s^3}{\mu_g}$	Abdullah et al., (2003)
$F_s = F_{s,0} x_c; Q_{ar} = Q_{mf,ar} (1 + \varepsilon_x) \frac{T}{T_0} \frac{P_0}{P}$	Scala e Salatino (2000)
$\frac{1}{D_{i,eff}} = \frac{\varepsilon_g}{\tau} \left(\frac{1}{D_{k,i}} + \frac{1}{D_{m,i}} \right); i = O_2, CO e CO_2$	Vasconcelos et al., (2003)
$\frac{1}{h_{gs}} = \frac{1}{h_g} + \frac{1}{h_s}; h_g = \frac{6 \lambda_{g,eff} Nu_s}{d_s^2}; h_s = \frac{2 \pi^2 k_{s,eff}}{9 d_s^2}$	Syamlal et al., (1993)
$Pr_g = \frac{C_{p,g} \mu_g}{\lambda_{g,eff}}; Re_s = \frac{d_s F_s - Q_{ar} \rho_g}{\mu_g}$	Syamlal et al., (1993)

Tabela 2 – Parâmetros Complementares para a simulação (Fan et al., 2003)

Parâmetros	Valores	Parâmetros	Valores	Parâmetros	Valores
d_s	183,356	$C_{p,g}$	$1,77 \times 10^3$	g	9,98
ρ_s	2530	$C_{p,s}$	$4,02 \times 10^3$	A_s	150
ρ_g	24	P	$2,1 \times 10^6$	R	8,314
μ_g	$1,14 \times 10^{-5}$	V_g	0,20	H	0,5
$\lambda_{g,eff}$	$2,49 \times 10^{-2}$	ΔH_j	$3,835 \times 10^6$	$\lambda_{s,eff}$	$3,76 \times 10^{-1}$
$T_{g,0}$	500°C	$T_{s,0}$	600°C	P_g	$2,1 \times 10^6$

The behaviour of variables T_g , T_s , Y_{O_2} , Y_{CO} , Y_{CO_2} , Y_{H_2O} and Y_C was shown in Figures (2), (3), (4), (5) and (6).

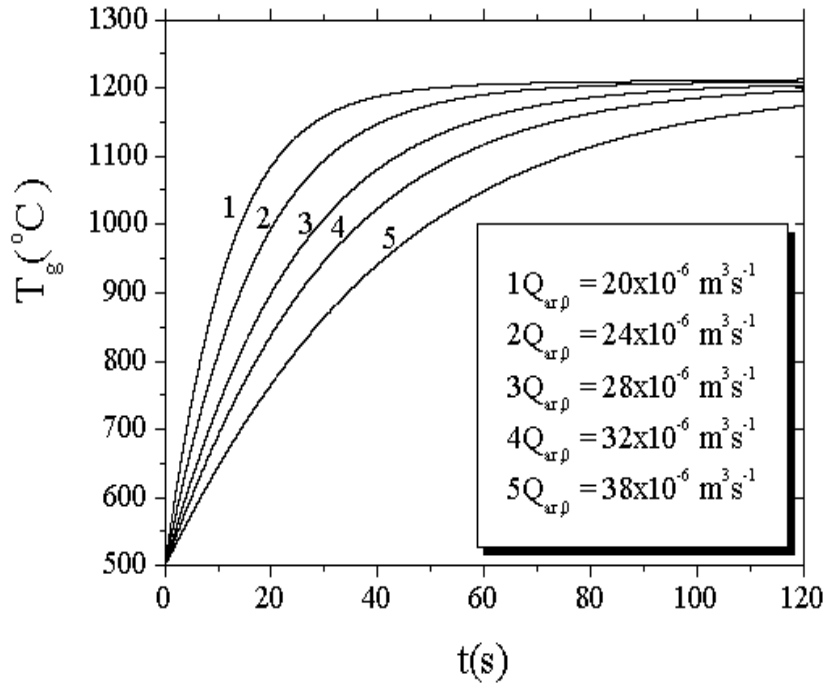


Figure 2: Temperature profiles of the gas phase for five different drainage at the entrance of gasifier

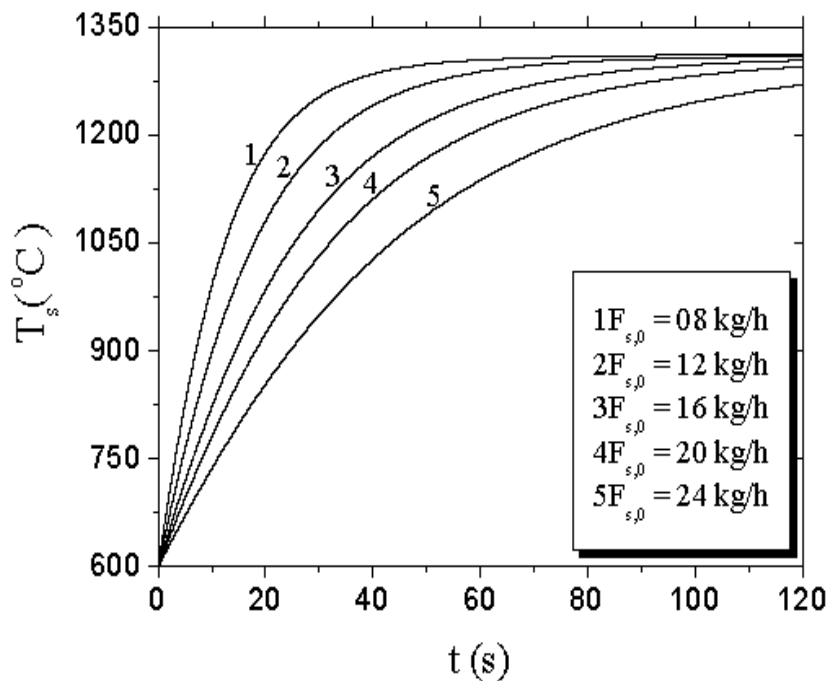


Figure 3: Temperature profiles of the solid phase for five different drainage at the entrance of gasifier.

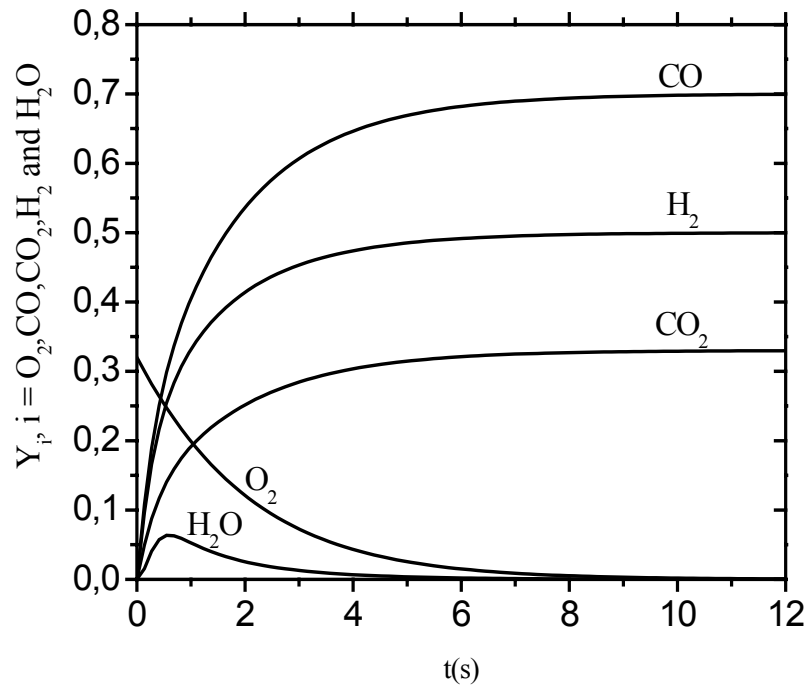


Figure 4: Behaviour of the molar fraction of components O_2 , CO , CO_2 , H_2 and H_2O .

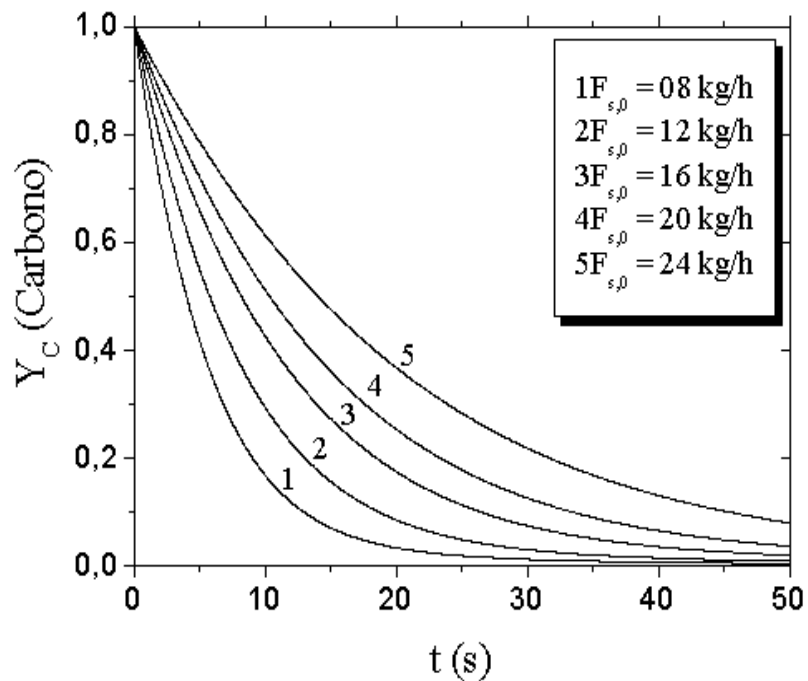


Figure 5: Behaviour of the molar fraction of the component C for five different drainage of the solid phase

Figures (2) and (3) shown the dynamic profiles of temperatures of the gas and solid phases at exit of the fluid-solid fluidization zone. It verified a substantial increase of temperatures T_g and T_s with the decrease of the gas and solid drainages at the entrance of gasifier. The Figure 2 shown that the temperature of gas reaches the stationary state in $t = \pm 60s$ for a gas drainage, $Q_{g,0} = 20 \times 10^{-4} \text{ m}^3 \text{ s}^{-1}$, reaching a temperature of $\pm 1200^\circ\text{C}$. The Figure (4) shows the behaviour of the reagent and product components of the gasification process. In Figure (5), it was analyzed the behaviour of the carbon component for five solid drainage. On the other hand, the Figure (6) shown a validation case.

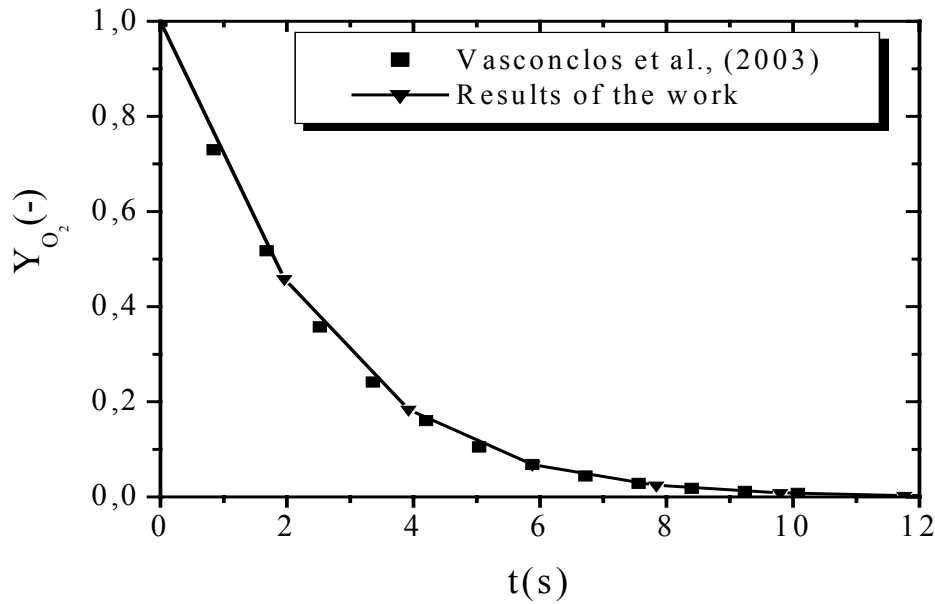


Figure 6: Validation of a numerical case with results of the literature

6. CONCLUSIONS

The forecasts of the behavior of temperatures of the gaseous phase and of the solid phase, as well as of the components O₂, CO, CO₂, H₂O, H₂ and C were shown in this work. For such end, it developed a mathematical model for variable T_g, T_s, Y_{O₂}, Y_{CO}, Y_{CO₂}, Y_{H₂O}, Y_{H₂} and Y_C. The simulation of the mathematical model supplied the behavior of these you varied, driving the following conclusions:

- The developed model allowed to analyze the sensibility of variable T_g with different drainage of entrance of the gas (Q_{ar,0}), as well as it allowed to verify the sensibility of variable T_s with different drainage of entrance F_{s,0}.
- The vazões Q_{ar,0} and F_{s,0} of entrance presented strong influence on variable T_g, T_s, Y_{O₂}, Y_{CO}, Y_{CO₂} and Y_C, should be consumed in the control of LF.

NOMENCLATURE

A _s	Gasifier cross area, m ²
C _{p,g}	Gas heat capacity, J/K mol
C _{p,s}	Solid heat capacity, J/K mol
D _{i,eff}	Effective diffusion coefficient, m ² /s
F _s	Mass flux of solid, kg/s
h _{gs}	Gas-solid transfer coefficient of solid, W/m ² K
ΔH _r	Entalpy of reaction, kJ/mol
Q _g	Total volumeter flow rate, m ³ /s
R _i	Reaction rates for the component, i = O ₂ , CO, CO ₂ , H ₂ O and H ₂ , s ⁻¹
t	time, s ⁻¹
T _g	Gas temperature, K
T _s	Solid temperature, K
Y _c	Molar fraction of carbon, dimensionless
Y _i	Molar fraction for the component i = O ₂ , CO, CO ₂ , H ₂ O and H ₂ , dimensionless

Greek Letters

ε _g	Volume fraction of gas, dimensionless
ε _s	Bed porosity, dimensionless
ρ _g	Gas density, kg/m ³
ρ _s	solid density, kg/m ³

$\lambda_{g,eff}$ Effective heat conductivity of gas, J/m s K
 $\lambda_{s,eff}$ Effective heat conductivity of solid, J/m s K

ACKNOWLEDGMENT

The main author of this work (Silva, J. D) thanks to CNPq (Conselho Nacional de Desenvolvimento) by the financial support given accordingly: (Processo 503711/2003-9/Projeto /Título: Desenvolvimento da Tecnologia de uma Unidade de Combustão Usando Bagaço de Cana e Resíduo Plástico para Produção de Energia Elétrica/Edital CT-Energ /CNPq /Proset 02/2003).

REFERENCES

- ABDULLAH, M. Z.; HUSAM, Z.; YIN PONG, S. L. ,(2003), “Analysis of coal flow fluidization test results for various biomass fuels, Biomass & Bioenergy, v. 24, p. 487-494.
- BASU, P., (1999), “Combustion of coal circulating fluidized-bed boilers: a review.” Chem. Eng. Sci, v. 54, p. 5545-5557.
- BROADHURST, T. E.; BECKER, H. A., (1975), “Onset of fluidization and slugging in beds of uniform particles, Aiche., v.21, p. 238-247
- CALLEJA, G.; SAROFIM, A. F.; GEORGAKIS, C., (1981),”Effect of char gasification order on the bounding solutions for char combustion”, Chem. Eng. Sci., v.36, p. 919-929.
- CUI, H. P.; MOSTOUFI, N.; CHAOUKI, J., (2000), “Characterization of dynamic gas-solid distribution in fluidized bed”, v. 79, p. 135.
- FAN, R.; MARCHISIO, D. L.; FOX, R. O. (2003) “CFD Simulation of polydisperse fluidized-bed polymerization reactors”, Sweeney hall, USA.
- GABRA, M.; PETTERSSON, E.; BACKMAN, R.; KJELLSTROM, B, (2001a), “Evaluation of cyclone gasifier performance for gasification of sugar cane residue-Part I: gasification of bagasse”, Biomass & Bioenergy, v. 21, p. 351-369.
- GABRA, M.; PETTERSSON, E.; BACKMAN, R.; KJELLSTROM, B., (2001b), “Evaluation of cyclone gasifier performance for gasification of sugar cane residue-Part I: gasification of cane trash”, Biomass & Bioenergy, v. 21, p. 371-380.
- Gabra, M.; Nordin, A.; Ohman, M.; Kjellstrom, B., (2001c), “Alkali retention/separation during bagasse gasification: a comparison between a fluidized bed and a cyclone gasifier”, Biomass & Bioenergy, v. 21, p. 461-476.
- GABRA, M.; SALMAN, H.; KJELLSTROM, B, (1998), “Development of a sugar cane residue feeding system for a cyclone gasifier”, Biomass & Bioenergy, v. 15, p. 143-153
- RICE, G.; DO, D. D., (1995), Applied Mathematics and Modeling for chemical engineers, John Wiley, cap. 7, p. 257.
- VASCONCELOS, S. M.; SILVA, J. D. ; LUCENA, S., (2003), Modelagem e simulação de um reator de leito fixo para produção de gás de síntese via oxidação parcial do gás”, 1º Congresso de P&D de Petróleo e Gás da UFPE, p. 342-347.
- SYAMLAL, M.; ROGERS, W.; O’BRIEN, T. J., (1993), MFX Documentation: Theory Guide, U. S. Department of Energy, Morgantown, West Virginia.
- SCALA, F.; SALATINO, P., (2000), “Modelling fluidized bed combustion of high-volatile solid fuels”, Chem. Eng. Sci, v. 57, p. 1175 – 1196.

APPENDIX-A

Table A1: Entrance and Parameter variables $\alpha_1, \alpha_2, \beta_1, \beta_2, \beta_3$ e β_4

$T_g _{z=0^-}(t) = T_{ent,g}$	$T_s _{z=0^-}(t) = T_{ent,s}$
$Y_{O_2,ar}(t) _{z=0^-} = Y_{O_2,ar}^0$	$Y_{CO,ar}(t) _{z=0^-} = Y_{CO,ar}^0$
$Y_{CO_2,ar}(t) _{z=0^-} = Y_{CO_2,ar}^0$	$Y_{C,ar}(t) _{z=0^-} = Y_{C,ar}^0$
$\alpha_1 = \frac{\rho_g C_{p,g} Q_{ar} \Delta z}{\lambda_{g,eff} A_s}$	$\alpha_2 = \frac{\rho_s C_{p,s} F_s \Delta z}{\lambda_{s,eff} A_s}$
$\beta_1 = \frac{Q_{ar}}{A_s} \frac{\Delta z}{D_{O_2,eff}}$	$\beta_2 = \frac{Q_{ar}}{A_s} \frac{\Delta z}{D_{CO,eff}}$
$\beta_3 = \frac{Q_{ar}}{A_s} \frac{\Delta z}{D_{CO_2,eff}}$	$\beta_4 = \frac{Q_{ar}}{A_s} \frac{\Delta z}{D_{C,eff}}$